Throughput Maximization in Buffer-aided Wireless-Powered NOMA Networks

Juanjuan Ren*, Xianfu Lei*, Fuhui Zhou†,
Panagiotis D. Diamantoulakis*‡, Octavia A. Dobre§, George K. Karagiannidis‡,
*School of Information Science and Technology, Southwest Jiaotong University, Chengdu, China
†College of Electronic and Information Engineering, Nanjing University of Aeronautics and Astronautics, Nanjing, China
‡Department of Electrical and Computer Engineering, Aristotle University of Thessaloniki, Thessaloniki, Greece
§Faculty of Engineering and Applied Science, Memorial University, St. John's, NL A1B 3X9, Canada
e-mails: juanjuanren@foxmail.com, xflei@swjtu.edu.cn, zhoufuhui@ieee.org,
padiaman@ieee.org, odobre@mun.ca, geokarag@auth.gr

***Abstract*—A new queue-length aware online scheduling scheme is proposed for a buffer-aided wireless-powered communication network (WPCN) with non-orthogonal multiple access (NOMA). The throughput of the considered network is maximized by designing the optimal resource allocation scheme, while preserving the stability of both energy and data queues. The formulated optimization problem is particularly challenging, since it is a long-term mixed-integer optimization problem. In order to solve it efficiently, we first transform the long-term optimization problem into a series of short-term ones at each time slot by taking advantage of the Lyapunov optimization framework, which can be efficiently solved. The analytical expression of the rate allocation reveals that in contrast to the case of WPCN without buffering, the optimal decoding order depends on the length of data buffer. Simulation results show that the proposed scheme outperforms the non-buffering scheme in terms of the long-term time-average sum rate.**

***Index Terms*—WPCN, buffer-aided, NOMA, Lyapunov optimization**

I. Introduction

Recently, wireless powered communication network (WPCN) has attracted increasing attention as one of the potential technologies to improve the lifetime of energy-constrained wireless networks [1]–[3]. WPCN can be implemented by using the ''harvest-then-transmit'' protocol [1], i.e., the hybrid access point (H-AP) first powers all users by broadcasting wireless energy during the downlink (DL) transmission, and then by using the harvested energy, users send information to the H-AP in the uplink (UL). In order to improve wireless information and power transfer efficiency, multi-antenna techniques are also widely considered in WPCN. For instance, the authors in [3] investigated a multiple-antenna power station model which can increase the wireless energy transfer efficiency and maximize the sum-throughput by jointly optimizing the time allocation factor and energy beamforming vector.

However, the above works considered users transmitting information in an orthogonal multiple access (OMA) manner; it is difficult to simultaneously meet the requirements of high spectrum efficiency and massive connectivity for Internet-of-Things applications. In order to address this issue, power-domain non-orthogonal multiple access (NOMA) which can serve multiple users in the same time/frequency/code resource was proposed [4]–[10]. In NOMA, advanced signal processing techniques are utilized in the decoding process to mitigate the intra-cell inter-user interference, such as successive interference cancellation (SIC). In [7], an uplink NOMA-enabled WPCN was studied, taking into account the decoding order of the user's messages. More specifically, time-sharing has been proposed for uplink NOMA, where multiple decoding orders for users are implemented for different portions of time, which enlarges the capacity region. It was shown that NOMA is superior to time division multiple access in terms of fairness, data rate that can be achieved by all users, as well as energy efficiency.

Moreover, with the substantial increasing demands for achieving higher throughput, data-buffer-aided communication has become an important technology [11]–[13], which can take advantage of the channels' ergodicity, as well as the knowledge of the channel state information (CSI) and the states of buffers to achieve higher average throughput. For instance, the authors in [11] considered a buffer-aided relay network and showed that data buffering can improve the throughput. In [12], an optimal power allocation and adaptive link selection scheme was proposed to improve the corresponding throughput. It is noted that most of the related works assumed that the harvested energy can be used immediately within one transmission block, which led to a poor performance in terms of long-term power consumption. To this end, when the channels undergo deep fading, an energy storage (e.g., battery or capacitor) is required, which can improve the power allocation efficiently by enabling the system to store the harvested energy.

Motivated by the above-mentioned facts, in this paper, data and energy buffers are explored in a wireless powered NOMA network. We first formulate a long-term time-average sum rate maximization problem, while guaranteeing the stability of all users' data and energy queues. Then, an online scheduling scheme based on the Lyapunov optimization framework [14] is proposed to solve the long-term stochastic optimization problem. Accordingly, control decisions and resource allocations are performed according to the real-time CSI and states of

978-1-7281-5089-5/20/$31.00 ©2020 IEEE

buffers. Furthermore, by deducing the analytic expression of the rate allocation, it is proved that the optimal decoding order of the users' messages in the considered system depends on the length of the data queues. Additionally, simulation results validate the effectiveness of the proposed algorithm and show that the proposed scheme outperforms the baseline one in terms of long-term time-average sum rate [7].

The remainder of this paper is organized as follows. In Section II, the system model is presented. Section III focuses on the design of optimal resource allocation for buffer-aided wireless-powered NOMA network. Simulation results are presented in Section IV, while Section V concludes the paper.

II. System Model

A buffer-aided wireless powered NOMA network is considered, as illustrated in Fig. 1. The network consists of one H-AP with K antennas and M users with a single antenna, denoted by U_m, $m \in \{1,2,...,M\}$. All users can harvest energy from the H-AP and send information to the H-AP in a NOMA manner. Moreover, each U_m is provisioned with a data buffer to store the received information from the upper layer and with an energy storage to store the harvested energy from the H-AP. Specifically, the H-AP transmits energy beams to all users in the DL, while in the UL, all energy-constrained users transmit the information to the H-AP in a NOMA manner by using the harvested RF energy.

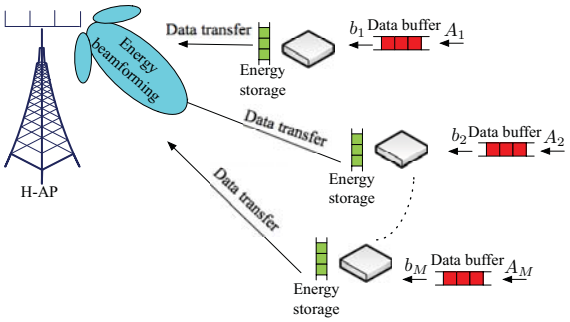

Fig. 1: Network model.

A time-slotted system is considered, and the duration of a time slot is denoted by T. $Q_m(t)$ and $E_m(t)$ are used to denote the available amount of data and energy for U_m in the corresponding data and energy buffer, respectively. Similar to [15], we also consider a flow controller at each U_m, and the upper layer traffic arrival process of U_m at time slot t is denoted by $A_m(t)$. Let $a_m(t)$ $(0 \le a_m(t) \le A_m(t))$ to denote the amount of data stored in the data buffer, and thus, the long-term time-average arrival rate can be described as

$$\overline{a}_m = \left(\lim_{N\to\infty} \frac{1}{N} \sum_{t=0}^{N-1} a_m(t) \right). \tag{1}$$

A. Channel Model

It is assumed that the channel coefficients are constant within one time slot but change independently from one time slot to another. Also, channel reciprocity is assumed. Let the complex random vector $\boldsymbol{g_m(t)} \in \mathbb{C}^{K\times 1}$ denote the small-scale Rayleigh fading between the H-AP and U_m at time slot t. The large-scale fading is also considered and the path loss exponent is denoted by α. Therefore, the channel coefficient vector can be described as $\tilde{\boldsymbol{g}}_{\boldsymbol{m}}(\boldsymbol{t}) = \frac{\boldsymbol{g_m(t)}}{\sqrt{d_m^{\alpha}}}$, where d_m is the transmit distance between the H-AP and U_m.

B. Communication Protocol

In the UL transmission mode, the information can be stored in the data buffer for several time slots if the channel conditions are not good. Moreover, the energy storage facilitates the users to exploit the harvested energy more efficiently, i.e., transmit information with a larger power level when the channel conditions are good. Furthermore, it is assumed that the H-AP can acquire the states of data and energy queues, as well as perfect CSI of all involved links. Thus, the system can switch between the following two modes at each time slot t.

Mode 1: Wireless energy beamforming mode. In this mode, the H-AP transmits the energy beamforming vector $\boldsymbol{w(t)} = (w_1(t), w_2(t), ..., w_K(t))^{\mathrm{T}} \in \mathbb{C}^{K\times 1}$ to all users. Hence, the transmit power of the H-AP can be described as

$$P(t) = ||\boldsymbol{w(t)}||^2 = \boldsymbol{w^H(t)w(t)}, \tag{2}$$

where the superscript $\boldsymbol{H}$ denotes the Hermitian transpose of the complex vector $\boldsymbol{w(t)}$ and the signal received at U_m can be expressed as

$$y_m(t) = \tilde{\boldsymbol{g}}_{\boldsymbol{m}}^{\boldsymbol{H}}\boldsymbol{(t)w(t)} + n_m(t), \tag{3}$$

where $n_m(t)$ is the additive white Gaussian noise (AWGN) at U_m with zero-mean and variance σ^2. We use $d(t) = 0$ and $d(t) = 1$ to represent the system state in **Mode 1** and **Mode 2**, respectively. Thus, the mode selection variable $d(t)$ satisfies

$$d(t) \in \{0,1\}, \forall t. \tag{4}$$

According to (3) and (4), the harvested energy of U_m at time slot t can be expressed as

$$H_m(t) = (1 - d(t))\,\eta\,|\tilde{\boldsymbol{g}}_{\boldsymbol{m}}^{\boldsymbol{H}}\boldsymbol{(t)w(t)}|^2 T, \tag{5}$$

where $\eta \in (0,1)$ is the energy conversion efficiency. The update equation of $E_m(t)$ is

$$E_m(t+1) = [E_m(t) + H_m(t) - P_m(t)T]^+, \tag{6}$$

where $[x]^+ = \max(0,x)$, and $\max(0,x)$ denotes the maximum value between 0 and x.

Mode 2: NOMA-aided wireless information transmission mode. In this mode, all users exploit the harvested energy in the energy storage to send information to the H-AP by using uplink NOMA. Thus, the received signal at the H-AP is

$$\boldsymbol{y}_{\mathrm{AP}}\boldsymbol{(t)} = \sum_{m=1}^{M} \sqrt{P_m(t)}\tilde{\boldsymbol{g}}_{\boldsymbol{m}}\boldsymbol{(t)}x_m(t) + \boldsymbol{n}, \tag{7}$$

where $P_m(t)$ is the transmit power of U_m, $\boldsymbol{I_K}$ denotes a $K \times K$ identity matrix and the complex Gaussian random variable

$\boldsymbol{n} \sim \mathcal{CN}(\mathbf{0}, \sigma^2 \boldsymbol{I_K})$ stands for noise at H-AP. Then, the H-AP decodes the information by using SIC. Thus, the transmission rate $\boldsymbol{R(t)} = \{R_1(t), R_2(t), ..., R_M(t)\}$ of users satisfies

$$\sum_{m\in S} R_m(t) \le \log_2\left(1 + \sum_{m\in S} ||\tilde{\boldsymbol{g}}_{\boldsymbol{m}}(\boldsymbol{t})||^2 P_m(t)\right), \forall m, \forall t, \quad (8)$$

where $S \subset \{1,2,...,M\}$ and $S \neq \varnothing$. It can be observed that (8) contains $2^M - 1$ constraints. The departure rate of the data buffer of U_m can be given as

$$b_m(t) = d(t) R_m(t) T, \forall m, \forall t. \quad (9)$$

Hence, the update equation of $Q_m(t)$ is given as

$$Q_m(t+1) = [Q_m(t) + a_m(t) - b_m(t)]^+. \quad (10)$$

III. Optimal Resource Allocation Scheme

In this section, we maximize the long-term time-average sum rate by designing an adaptive scheduling scheme. Mode selection, rate control, energy beamforming, rate and power allocations are jointly considered to achieve the goal. The optimization problem can be formulated as

$$\mathbf{P}_1: \max_{\substack{d(t),\mathbf{P(t)},\\ \mathbf{R(t)},\mathbf{a(t)},\mathbf{w(t)}}} \sum_{m=1}^{M} \bar{a}_m \quad (11a)$$

$$\text{s.t. } \mathrm{C}_1: 0 \le a_m(t) \le A_m(t), \forall m, \forall t, \quad (11b)$$

$$\mathrm{C}_2: \sum_{m\in S} R_m(t) \le \log_2\left(1 + \sum_{m\in S} ||\tilde{\boldsymbol{g}}_{\boldsymbol{m}}(\boldsymbol{t})||^2 P_m(t)\right), \forall m, \forall t, \quad (11c)$$

$$\mathrm{C}_3: 0 \le P_m(t) \le \hat{P}_m(t), \forall m, \forall t, \quad (11d)$$

$$\mathrm{C}_4: 0 \le ||\boldsymbol{w(t)}||^2 \le \hat{P}_{\mathrm{AP}}(t), \forall t, \quad (11e)$$

$$\mathrm{C}_5: \lim_{N\to+\infty} \frac{1}{N} \sum_{t=0}^{N-1} (1 - d(t)) ||\boldsymbol{w(t)}||^2 \le \bar{P}_{\max} T, \quad (11f)$$

$$\mathrm{C}_6: d(t)(1 - d(t)) = 0, \forall t, \quad (11g)$$

$$\mathrm{C}_7: \bar{a}_m \le \lim_{N\to\infty} \frac{1}{N} \sum_{t=0}^{N-1} d(t) R_m(t) T, \forall m, \quad (11h)$$

$$\mathrm{C}_8: \lim_{N\to\infty} \frac{1}{N} \sum_{t=0}^{N-1} d(t) P_m(t) T \le \lim_{N\to\infty} \frac{1}{N} \sum_{t=0}^{N-1} H_m(t), \forall m, \quad (11i)$$

where $\mathbf{P(t)} = [P_1(t), P_2(t), ..., P_M(t)]$, $\mathbf{R(t)} = [R_1(t), R_2(t), ..., R_M(t)]$ and $\mathbf{a(t)} = [a_1(t), a_2(t), ..., a_M(t)]$. $\bar{P}_{\max}$ denotes the average power budget at H-AP, and the maximum instantaneous transmit power of the H-AP and U_m are $\hat{P}_{\mathrm{AP}}(t)$ and $\hat{P}_m(t)$, respectively. In particular, C_1 and C_2 describe the arrival and departure rate constraints. The instantaneous power constrains of U_m and H-AP can be guaranteed by C_3 and C_4, respectively. The average power budget at H-AP is guaranteed by C_5. Moreover, C_6 indicates that the system only selects one of the two modes in each time slot t. Finally, the stability of the corresponding data and energy queues are ensured by C_7 and C_8, respectively.

It is noted that the optimization problem (11) is not only a mixed-integer programming problem due to C_6, but also contains long-term time-average terms. Thus, it is particularly challenging to solve this with acceptable complexity. To this end, we propose an online algorithm by exploring the Lyapunov optimization framework [14].

In order to solve (11), we first convert C_5 into the stability of virtual queue $E_{\mathrm{AP}}(t)$ as follows

$$E_{\mathrm{AP}}(t+1) = \left[E_{\mathrm{AP}}(t) + (1 - d(t)) ||\boldsymbol{w(t)}||^2 T - \bar{P}_{\max} T\right]^+, \quad (12)$$

where $\bar{P}_{\max} T$ and $(1 - d(t)) ||\boldsymbol{w(t)}||^2$ correspond to the departure rate and arrival rate of the queue, respectively. In Lemma 1 below, we prove that the constraint C_5 is equivalent to keeping the stability of the queue $E_{\mathrm{AP}}(t)$.

Lemma 1: If $E_{\mathrm{AP}}(t)$ is mean rate stable, i.e., $\lim_{t\to+\infty} \frac{E_{\mathrm{AP}}(t)}{t} = 0$, then long-term time-average power constraint C_5 of the H-AP can be guaranteed.

Proof: According to (12), one has

$$E_{\mathrm{AP}}(t+1) \ge E_{\mathrm{AP}}(t) + (1 - d(t)) ||\boldsymbol{w(t)}||^2 T - \bar{P}_{\max} T. \quad (13)$$

Summing (13) over t and dividing by t, we have

$$\frac{E_{\mathrm{AP}}(t) - E_{\mathrm{AP}}(0)}{t} \ge \frac{1}{t} \sum_{l=0}^{t-1} (1 - d(t)) ||\boldsymbol{w(t)}||^2 T - \bar{P}_{\max} T. \quad (14)$$

By assuming that the initial state of $E_{\mathrm{AP}}(t)$ is zero and combining with $\lim_{t\to+\infty} \frac{E_{\mathrm{AP}}(t)}{t} = 0$, one has

$$(1 - d(t)) ||\boldsymbol{w(t)}||^2 T \le \bar{P}_{\max} T. \quad (15)$$

The proof is completed. ■

Similarly, C_7 and C_8 can also be converted into the stability problem of the corresponding data and energy queues, respectively. Now, the long-term constraints C_5, C_7 and C_8 in optimization problem (11) can be transformed into the problem of keeping the stability of queues.

We describe the queues by defining the following queue backlog vector

$$\boldsymbol{\Theta}(t) = [\boldsymbol{Q(t)}, \boldsymbol{E(t)}, E_{\mathrm{AP}}(t)], \quad (16)$$

where $\boldsymbol{Q(t)} = [Q_1(t), Q_2(t), ..., Q_M(t)]$ and $\boldsymbol{E(t)} = [E_1(t), E_2(t), ..., E_M(t)]$. Thus, the size of $\boldsymbol{\Theta}(t)$ is

$$L(\boldsymbol{\Theta}(t)) = \frac{1}{2} \sum_{m=1}^{M} \mu_{1m} Q_m^2(t) + \frac{1}{2} \sum_{m=1}^{M} \mu_{2m} (\phi_m - E_m(t))^2 + \frac{\mu_3}{2} E_{\mathrm{AP}}^2(t). \quad (17)$$

In order to keep the stability of all queues, the positive weight factors μ_{1m}, μ_{2m} and μ_3 are introduced. ϕ_m is the perturbation value of $E_m(t)$, and it is assumed that $E_m(t) \le \phi_m$ [13]. Thus, we can modify the update equation of $E_m(t)$ as

$$E_m(t+1) = \min\{E_m(t) + H_m(t) - P_m(t) T, \phi_m\}. \quad (18)$$

Next, the one-slot conditional Lyapunov drift function is defined as

$$\Delta(\boldsymbol{\Theta}(t)) \triangleq \mathbb{E}\{L(\boldsymbol{\Theta}(t+1)) - L(\boldsymbol{\Theta}(t)) | \boldsymbol{\Theta}(t)\}, \quad (19)$$

which characterizes the increment of $L(\boldsymbol{\Theta}(t))$. By minimizing

$\Delta(\mathbf{\Theta}(t))$, the stability of the queues can be ensured [14]. Moreover, we aim for maximizing the time-average sum function. Therefore, following the Lyapunov optimization framework, we should minimize the drift-minus-utility function, given as

$$\Delta(\mathbf{\Theta}(t)) - V\sum_{m=1}^{M} a_m(t), \tag{20}$$

where $V \geq 0$ is a non-negative penalty weight that is chosen to control the tradeoff between the optimum performance and the average queue size.

Lemma 2: For given $\mathbf{\Theta}(t)$ and V, it is assumed that the channel gain is independent and identically distributed over different time slots. The upper bound of (20) is given as

$$\begin{aligned}
&\Delta(\mathbf{\Theta}(t)) - V\sum_{m=1}^{M} a_m(t) \\
\leq& B - V\sum_{m=1}^{M} a_m(t) + \sum_{m=1}^{M} \mu_{1m} Q_m(t)\mathbb{E}\left\{a_m(t) - b_m(t)|\mathbf{\Theta}(t)\right\} \\
&+ \sum_{m=1}^{M} \mu_{2m}(\phi_m - E_m(t))\mathbb{E}\left\{d(t)P_m(t)T - H_m(t)|\mathbf{\Theta}(t)\right\} \\
&+ \mu_3 E_{\mathrm{AP}}(t)\mathbb{E}\left\{(1-d(t))\,||\boldsymbol{w}(\boldsymbol{t})||^2 - \bar{P}_{\max}|\mathbf{\Theta}(t)\right\},
\end{aligned} \tag{21}$$

where B is a constant, given as

$$\begin{aligned}
B = &\frac{1}{2}\mathbb{E}\left\{\sum_{m=1}^{M}(\mu_{1m}\hat{a}_m)^2 + (\mu_{1m}\hat{b}_m)^2 + (\mu_{2m}\hat{H}_m)^2 + (\mu_{2m}\hat{P}_m)^2\right\} \\
&+ \frac{1}{2}\mathbb{E}\left\{\left(\mu_3\hat{P}_{\mathrm{AP}}\right)^2 + \left(\mu_3\bar{P}_{\max}\right)^2\right\},
\end{aligned} \tag{22}$$

where $\hat{a}_m$, $\hat{b}_m$, and $\hat{H}_m$ are the maximum values of $a_m(t)$, $b_m(t)$, and $H_m(t)$, respectively.

Proof: According to the data queue update equation (10), we first find the upper bound of $Q_m^2(t+1) - Q_m^2(t)$ as

$$\begin{aligned}
&Q_m^2(t+1) - Q_m^2(t) \\
=&\left([Q_m(t) + a_m(t) - b_m(t)]^+\right)^2 - Q_m^2(t) \\
\leq&\left(Q_m(t) + a_m(t) - b_m(t)\right)^2 - Q_m^2(t) \\
=&\left(a_m(t) - b_m(t)\right)^2 + 2Q_m(t)\left(a_m(t) - b_m(t)\right) \\
\leq&a_m^2(t) + b_m^2(t) + 2Q_m(t)\left(a_m(t) - b_m(t)\right) \\
\leq&\hat{a}_m^2 + \hat{b}_m^2 + 2Q_m(t)\left(a_m(t) - b_m(t)\right).
\end{aligned} \tag{23}$$

Thus, one has

$$\frac{Q_m^2(t+1) - Q_m^2(t)}{2} \leq \frac{\hat{a}_m^2 + \hat{b}_m^2}{2} + Q_m(t)\left(a_m(t) - b_m(t)\right). \tag{24}$$

In a similar way, it holds that

$$\begin{aligned}
\frac{E_m^2(t+1) - E_m^2(t)}{2} \leq &\frac{\hat{H}_m^2 + \hat{P}_m^2}{2} + (\phi_m - E_m(t)) \times \\
&\left(d(t)P_m(t)T - H_m(t)\right),
\end{aligned} \tag{25}$$

$$\begin{aligned}
\frac{E_{\mathrm{AP}}^2(t+1) - E_{\mathrm{AP}}^2(t)}{2} \leq &\frac{\hat{P}_{\mathrm{AP}}^2 + (\bar{P}_{\max})^2}{2} + E_{\mathrm{AP}}(t) \times \\
&\left((1-d(t))||\boldsymbol{w}(\boldsymbol{t})||^2 - \bar{P}_{\max}T\right).
\end{aligned} \tag{26}$$

By taking conditional expectations over the above four equations, and adding $V\sum_{m=1}^{M} a_m(t)$ to both sides, the proof is completed. ■

In order to maximize the objective function while keeping the stability of all involved queues, we should try to minimize the upper bound of the Lyapunov drift-minus-penalty item given by Lemma 2. Thus, for given queue states and CSI at current slot, one obtains the following optimization problem

$$\begin{aligned}
\mathbf{P}_2: \min_{\substack{d(t),\mathbf{P}(\mathbf{t}),\\ \mathbf{R}(\mathbf{t}),\mathbf{a}(\mathbf{t}),\mathbf{w}(\mathbf{t})}} \quad &-V\sum_{m=1}^{M} a_m(t) + \sum_{m=1}^{M} \mu_{1m} Q_m(t)\left(a_m(t) - b_m(t)\right) \\
&+ \sum_{m=1}^{M} \mu_{2m}\left(\phi_m - E_m(t)\right)\left(d(t)P_m(t)T - H_m(t)\right) \\
&+ \mu_3 E_{\mathrm{AP}}(t)\left((1-d(t))\,||\boldsymbol{w}(\boldsymbol{t})||^2 - \bar{P}_{\max}\right) \quad (27a) \\
\text{s.t. } &\mathrm{C}_1 \sim \mathrm{C}_5, \mathrm{C}_7. \quad (27b)
\end{aligned}$$

Taking into account the special structure of the optimization problem (27), it can be divided into four-subproblems as follows, namely,

Arrival rate control: It is observed that $a_m(t)$ is independent of the other variables, and thus, we can obtain the following optimization problem related to $\mathbf{a}(\mathbf{t})$:

$$\begin{aligned}
\mathbf{P}_3: \quad &\min_{\mathbf{a}(\mathbf{t})} \sum_{m=1}^{M} \left(\mu_{1m} Q_m(t) - V\right) a_m(t) \quad (28a) \\
&\text{s.t. } \mathrm{C}_1. \quad (28b)
\end{aligned}$$

It can be seen that (28) is a linear programming. Thus, the optimal value of $a_m(t)$ can be obtained at the boundaries of the constraint C_1, i.e.,

$$a_m(t) = \begin{cases} A_m(t), & \text{if } \mu_{1m} Q_m(t) < V, \\ 0, & \text{otherwise.} \end{cases} \tag{29}$$

It can be observed that all of the new generated data are admitted if the queue length at the current slot is smaller than the threshold V; otherwise, there is too much data in the corresponding data queue, and thus, no new data will be placed into the corresponding data buffer. In other words, the arrival rate control policy is a queue length threshold-based one.

In order to obtain the optimal mode selection scheme, we first consider the following sub-problem-2 and sub-problem-3, which correspond to wireless energy beamforming mode and NOMA-aided wireless information transmission mode, respectively.

Energy beamforming optimization: In this subproblem, the system performs energy transfer, i.e., $d(t) = 0$, and thus, the optimization problem corresponding to this mode can be formulated as

$$\begin{aligned}
\mathbf{P}_4: \quad &\min_{\boldsymbol{w}(\boldsymbol{t})} -\sum_{m=1}^{M} \mu_{2m}\left(\phi_m - E_m(t)\right) H_m(t) + \mu_3 E_{\mathrm{AP}}(t) \times \\
&\left(||\boldsymbol{w}(\boldsymbol{t})||^2 - \bar{P}_{\max}\right) \quad (30a) \\
&\text{s.t. } \mathrm{C}_5. \quad (30b)
\end{aligned}$$

The optimal energy beamforming vector is

$$\boldsymbol{w(t)} = \begin{cases} 0, & \text{if } d_{min}(t) \geq 0, \\ \sqrt{\hat{P}(t)}\boldsymbol{u_1(t)}, & \text{otherwise}, \end{cases} \tag{31}$$

where $d_{\min}(t)$ is the smallest eigenvalue of $D(t) = \mu_3 E_{\mathrm{AP}}(t) I - \sum_{m=1}^{M} \mu_{2m} (\phi_m - E_m(t)) \eta T G_m(t)$ and $\boldsymbol{u_1(t)}$ denotes the eigenvector corresponding to $d_{\min}(t)$.

Proof: Substituting (5) into the objective function of (30), we can get the following optimization problem

$$\begin{aligned} \mathbf{P}_5: \min_{\boldsymbol{w(t)}} & -\sum_{m=1}^{M} \mu_{2m} (\phi_m - E_m(t)) \eta |(\tilde{\boldsymbol{g}}_{\boldsymbol{m}}(\boldsymbol{t}))^H \boldsymbol{w(t)}|^2 T + \\ & \mu_3 E_{\mathrm{AP}}(t) \left(||\boldsymbol{w(t)}||^2 - \bar{P}_{max} \right) && \text{(32a)} \\ \text{s.t.} \quad & \mathrm{C}_5. && \text{(32b)} \end{aligned}$$

Next, letting $G_m(t) = \tilde{\boldsymbol{g}}_{\boldsymbol{m}}(\boldsymbol{t}) \tilde{\boldsymbol{g}}_{\boldsymbol{m}}^{\boldsymbol{H}}(\boldsymbol{t})$ and $W(t) = \boldsymbol{w(t)} \boldsymbol{w^H(t)}$, and thus, (32) can be rewritten as

$$\begin{aligned} \mathbf{P}_6: \min_{W(t)} & -\sum_{m=1}^{M} \mu_{2m} (\phi_m - E_m(t)) \eta \mathrm{tr}(G_m(t) W(t)) T \\ & + \mu_3 E_{\mathrm{AP}}(t) \mathrm{tr}(W(t)) && \text{(33a)} \\ \text{s.t.} \quad & \mathrm{C}_1: 0 \leq \mathrm{tr}(W(t)) \leq \hat{P}, \forall t, && \text{(33b)} \\ & \mathrm{C}_2: \mathrm{rank}(W(t)) = 1, \forall t, && \text{(33c)} \\ & \mathrm{C}_3: W(t) \in S_+^K, \forall t, && \text{(33d)} \end{aligned}$$

Let $D(t) = \mu_3 E_{AP}(t) I - \sum_{m=1}^{M} \mu_{2m} (\phi_m - E_m(t)) \eta T G_m(t)$, then the objective function of (33) can be rewritten as $\mathrm{tr}(D(t)W(t))$. Based on the fact that

$$\begin{aligned} \mathrm{tr}(D(t)W(t)) &= \mathrm{tr}(U(t) \sum_{D} U^H(t) V(t) \sum_{W} V^H(t)) && \text{(34a)} \\ &= \mathrm{tr}(V^H(t) U(t) \sum_{D} U^H(t) V(t) \sum_{W}) && \text{(34b)} \\ &= \mathrm{tr}(M(t) \sum_{D} M^H(t) \sum_{W}) && \text{(34c)} \\ &= W_1(t) \sum_{i=1}^{K} d_i(t) M_{1i}^2(t), && \text{(34d)} \end{aligned}$$

where (34b) follows from the fact that $\mathrm{tr}(AB) = \mathrm{tr}(BA)$, (34c) can be obtained by letting $M(t) = V^H(t) U(t)$ and (34c) is deduced by following $\mathrm{rank}(W(t)) = 1$.

One can get

$$\begin{aligned} \mathbf{P}_7: \min_{W_1(t)} & \; W_1(t) \sum_{i=1}^{K} d_i(t) M_{1i}^2(t) && \text{(35a)} \\ \text{s.t.} \quad & \sum_{i=1}^{K} M_{1i}^2(t) = 1, \forall t, && \text{(35b)} \end{aligned}$$

by some briefly discussing of (35), we can get the results. ■

Transmission power and rate allocation: In this subproblem, the system operates in information transfer mode, i.e., $d(t) = 1$, thus, the optimization problem in this mode can be expressed as

$$\begin{aligned} \mathbf{P}_8: \min_{\boldsymbol{R(t)}, \boldsymbol{P(t)}} & -\sum_{m=1}^{M} \mu_{1m} Q_m(t) R_m(t) T + \sum_{m=1}^{M} \mu_{2m} (\phi_m - E_m(t)) P_m(t) T && \text{(36a)} \\ \text{s.t.} \quad & \mathrm{C}_3, \mathrm{C}_4. && \text{(36b)} \end{aligned}$$

In order to make more clear the analysis of (36), the data buffers are sorted in an ascending order depending on their lengths, i.e.,

$$0 < \mu_{1(A(j_1))} Q_{A(j_1)} \leq \mu_{1(A(j_2))} Q_{A(j_2)} \cdots \leq \mu_{1(A(j_L))} Q_{A(j_L)}. \tag{37}$$

We use $\Omega = \{A(j_1), A(j_2), ..., A(j_L)\}$ to denote the set of non-empty data buffers, and then, (36) can be reformulated as

$$\begin{aligned} \mathbf{P}_9: \min_{\boldsymbol{R_\Omega(t)}, \boldsymbol{P_\Omega(t)}} & -\sum_{l=1}^{L} \mu_{1(A(j_l))} Q_{A(j_l)}(t) R_{A(j_l)}(t) T + \sum_{l=1}^{L} \mu_{2(A(j_l))} \\ & \times \left(\phi_{A(j_l)} - E_{A(j_l)}(t) \right) P_{A(j_l)}(t) T && \text{(38a)} \\ \text{s.t.} \; \mathrm{C}_1: & \sum_{A(j_l) \in S} R_{A(j_l)}(t) \leq \log_2 \Big(1 + \sum_{A(j_l) \in S} ||\tilde{\boldsymbol{g}}_{A(j_l)}(\boldsymbol{t})||^2 \\ , & \qquad \times P_{A(j_l)}(t) \Big), \; S \subseteq \Omega, \forall t, \\ & \mathrm{C}_2: 0 \leq P_{A(j_l)}(t) \leq \hat{P}_{A(j_l)}(t), \forall A(j_l), \forall t, && \text{(38b)} \end{aligned}$$

where $\boldsymbol{R_\Omega(t)} = \left[R_{A(j_1)}(t), R_{A(j_2)}(t), ..., R_{A(j_L)}(t) \right]$ and $\boldsymbol{P_\Omega(t)} = \left[P_{A(j_1)}(t), P_{A(j_2)}(t), ..., P_{A(j_L)}(t) \right]$. Next, we expand the first item of the objective function in (38), thus, (38) can be rewritten as

$$\begin{aligned} \mathbf{P}_{10}: \min_{\boldsymbol{R_\Omega(t)}, \boldsymbol{P_\Omega(t)}} & -\sum_{l=1}^{L} \Bigg[\left(\mu_{1(A(j_l))} Q_{A(j_l)}(t) - \mu_{1A(j_{(l-1)})} Q_{A(j_{(l-1)})}(t) \right) && \text{(39a)} \\ & \times \sum_{p=l}^{L} R_p(t) \Bigg] T + \sum_{l=1}^{L} \mu_{2(A(j_l))} \left(\phi_{A(j_l)} - E_{A(j_l)}(t) \right) P_{A(j_l)}(t) T && \text{(39b)} \\ \text{s.t.} \; \mathrm{C}_1: & \sum_{A(j_l) \in S} R_{A(j_l)}(t) \leq \log_2 \Big(1 + \sum_{A(j_l) \in S} ||\tilde{\boldsymbol{g}}_{A(j_l)}(\boldsymbol{t})||^2 \\ , & \qquad \times P_{A(j_l)}(t) \Big), \; S \subseteq \Omega, \forall t, \\ & \mathrm{C}_2: 0 \leq P_{A(j_l)}(t) \leq \hat{P}_{A(j_l)}(t), \forall A(j_l), \forall t, && \text{(39c)} \end{aligned}$$

Since the coefficient of $\sum_{p=l}^{L} R_p(t)$ is negative, i.e., the objective function is a monotonically decreasing function of $\sum_{p=l}^{L} R_p(t)$. Thus, the optimal solution for $R_\Omega(t)$ is achieved at the equal terms in C_1, i.e.,

$$R_{A(j_l)} = \log_2 \left(1 + \frac{P_{A(j_l)} ||\tilde{\boldsymbol{g}}_{A(j_l)}(\boldsymbol{t})||^2}{1 + \sum_{A(j_k) \in \{\Omega / A(j_1), A(j_2), ..., A(j_l)\}} P_{A(j_k)} ||\tilde{\boldsymbol{g}}_{A(j_k)}(\boldsymbol{t})||^2} \right). \tag{40}$$

It can be observed that the H-AP performs a queue-length aware SIC, i.e., the user with the longest queue decodes its own information without suffering interference. This SIC scheme can be explained as that the user with more backlog in its data

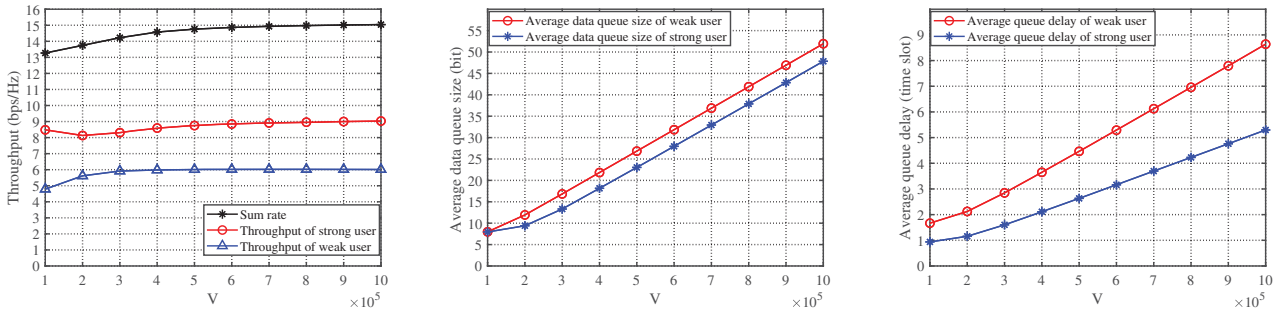

(a) Throughout of each user vs. V. (b) Average data queue size of each user vs. V. (c) Average queue delay of each user vs. V.

Fig. 2: Performance of the proposed scheme.

buffer should have a higher transmit rate. Then, substituting the expression of $R_{A(j_l)}$ into (38), we have

$$\mathbf{P}_{11}: \min_{P_{\Omega}(t)} \sum_{l=1}^{L} \mu_{2A(j_l)} \left(\phi_{A(j_l)} - E_{A(j_l)}(t)\right) P_{A(j_l)}(t)T$$
$$-\sum_{l=1}^{L} \mu_{1(A(j_l))} Q_{A(j_l)}(t) T \log_2 \left(1+ \right. \tag{41a}$$
$$\left. \frac{P_{A(j_l)} ||\tilde{\boldsymbol{g}}_{A(j_l)}(\boldsymbol{t})||^2}{1+\sum\limits_{A(j_k)\in\{\Omega/A(j_1),A(j_2),\ldots,A(j_l)\}} P_{A(j_k)} ||\tilde{\boldsymbol{g}}_{A(j_k)}(\boldsymbol{t})||^2}\right) \tag{41b}$$
$$\text{s.t. } \mathrm{C}_1: 0 \le P_{A(j_l)}(t) \le \hat{P}_{A(j_l)}(t), \forall A(j_l), \forall t. \tag{41c}$$

It can be seen that (41) is a convex optimization problem due to the convexity of the objective function and the linearity of the constraints. Thus, we use the interior point method to solve it efficiently.

Optimal mode selection: By observing the above analysis, it can be concluded that the optimal mode selection scheme is

$$d^*(t) = \begin{cases} 1, & \text{if} \quad A^*(t) = \arg\min_{i=1,2} A_i^*(t), \\ 0, & \text{otherwise}, \end{cases} \tag{42}$$

where $A_1^*(t)$ and $A_2^*(t)$ are

$$A_1^*(t) = -\sum_{m=1}^{M} \mu_{2m} \left(\phi_m - E_m(t)\right) H_m(t) + \mu_3 E_{\mathrm{AP}}(t) \times$$
$$\left(||\boldsymbol{w}^*(\boldsymbol{t})||^2 - \bar{P}_{\max}\right), \tag{43a}$$
$$A_2^*(t) = -\sum_{m=1}^{M} \mu_{1m} Q_m(t) R_m^*(t) T + \sum_{m=1}^{M} \mu_{2m} (\phi_m - E_m(t)) P_m^*(t) T. \tag{43b}$$

A. Performance Analysis

In this subsection, the analytical bounds of the long-term time-average sum rate, and the buffer length in our scheme are presented in the following theorem.

Theorem 1: For arbitrary $V > 0$, there exist constants $\varepsilon > 0$ and $B > 0$, such that the proposed policy satisfies the following properties:

$$U_m^* - \frac{B}{V} \le \sum_{m=1}^{M} \bar{a}_m \le U_m^*, \tag{44}$$

$$\lim_{T\to+\infty} \frac{1}{T} \sum_{t=0}^{T-1} \sum_{m=1}^{M} \mathbb{E}\{Q_m(t)\} \le \frac{B + V\left[U_m^* - \Psi(\varepsilon)\right]}{\varepsilon}, \tag{45}$$

where U_m^* is the theoretical optimal value of $\sum_{m=1}^{M} \bar{a}_m$ and $\Psi(\varepsilon)$ is a constant.

The proof of Theorem 1 is similar to the proof of Theorem 4.2 in [14]. Theorem 1 shows that the proposed scheme can ensure the stability of buffers, and the achievable sum rate arbitrarily approaches U_m^* by increasing V, while the length of the data buffer increases linearly. In other words, there exists a tradeoff $[O(V), O(1/V)]$ between the queue backlog and the gap to the theoretical optimal sum rate. Moreover, the computational complexity of the proposed scheme is roughly $O\left(n^{3.5}\right)$, which comes mainly from the interior point method used for solving $P_m(t)$.

IV. Simulation Results and Discussion

In this section, we present the simulation results. The average transmission power budget and the noise variances of the H-AP are considered as $\bar{P}_{\max} = 30$ dBm and -100 dBm, respectively. The energy harvesting efficiency is set to $\eta = 0.5$. It is assumed that $g_{m,i}$ follows the Rayleigh distribution. We set the path loss exponent to $\alpha = 2$. Moreover, we assume that the data arrival rate $A_m(t)$ follows the Poisson process with mean value $A_{\mathrm{av}} =$ 15 bps. Finally, the scheme in [7] is the baseline scheme, which considers a WPCN with NOMA but without buffering.

We first present the performance of the proposed scheme in Fig. 2. The user locations are set as $d_1 = 5$ m, $d_2 = 10$ m, $\theta_1 = 0^\circ$ and $\theta_2 = 45^\circ$. Fig. 2 (a) shows that the throughput of the near and far users gradually increases with V, respectively, which is consistent with (44). It is also seen that the throughput of the near user firstly decreases before achieving stability, which is consistent with the characteristic of NOMA. From Fig. 2 (b) and Fig. 2 (c), we see that with the increase of V, the average buffer size and delay of each user increase linearly, which is consistent with the analysis of (45).

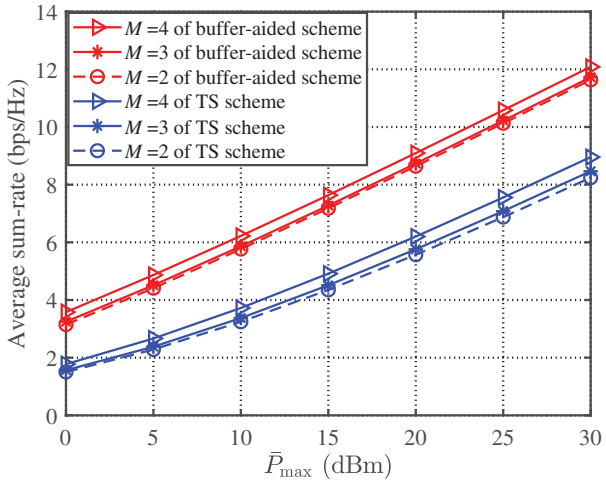

Fig. 3: The throughput vs. the average power budget at H-AP.

In Fig. 3, the long-term average sum-rate of all users is illustrated with different values of M, e.g., 2, 3, 4. It is seen that our scheme is superior to the non-buffering scheme [7], which implies that the proposed adaptive scheduling scheme can increase the system performance by taking full advantage of the extra degrees of freedom introduced by the data and energy buffers. Fig. 4 illustrates that as the number of antennas increases, the long-term average sum-rate and the long-term average rate of the user that achieves the lowest average rate can be gradually increased, and the gain comes from the spatial gain owing to multiple antennas at H-AP.

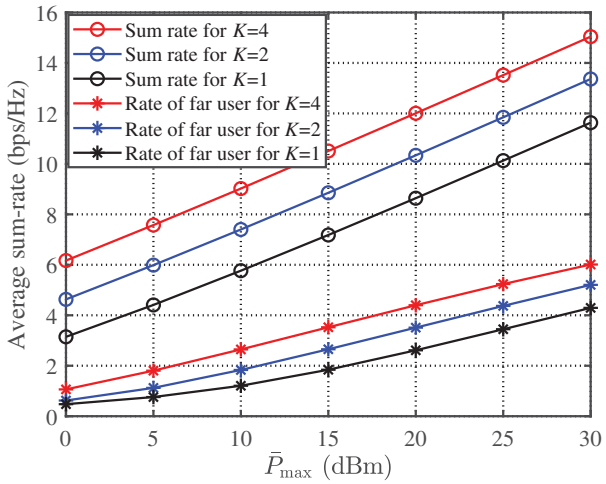

Fig. 4: The throughput vs. different number of antennas at H-AP.

V. Conclusions

In this paper, the long-term time-average sum rate of the buffer-aided wireless-powered NOMA network with a multi-antenna H-AP was investigated. Results revealed that the optimal decoding order depends on the lengths of the data buffers, which is different from that in the wireless-powered NOMA network without buffering. Moreover, it was seen that the proposed scheme can obtain the asymptotically optimal solution with a low computational complexity. Finally, simulation results demonstrated that the proposed scheduling policy can significantly improve the long-term time-average sum rate compared with the non-buffering scheme.

Acknowledgment

This work was supported by the Sichuan Science and Technology Program under Grant 2017HH0035, the NSFC project under Grant 61971360/61701214, the Fundamental Research Funds for the Central Universities under Grant 2682018CX27, the Excellent Youth Foundation of Jiangxi Province under Grant 2018ACB21012, and the Young Elite Scientist Sponsorship Program by CAST.
(Xianfu Lei is the corresponding author of this paper.)

References

[1] H. Ju and R. Zhang, "Throughput maximization in wireless powered communication networks," *IEEE Trans. Wireless Commun.*, vol. 13, no. 1, pp. 418–428, Jan. 2014.
[2] Z. Hadzi-Velkov, I. Nikoloska, G. K. Karagiannidis, and T. Q. Duong, "Wireless networks with energy harvesting and power transfer: Joint power and time allocation," *IEEE Signal Process. Lett.*, vol. 23, no. 1, pp. 50–54, Jan. 2016.
[3] Q. Sun, G. Zhu, C. Shen, X. Li, and Z. Zhong, "Joint beamforming design and time allocation for wireless powered communication networks," *IEEE Commun. Lett.*, vol. 18, no. 10, pp. 1783–1786, Oct. 2014.
[4] Y. Saito, Y. Kishiyama, A. Benjebbour, T. Nakamura, A. Li, and K. Higuchi, "Non-orthogonal multiple access (noma) for cellular future radio access," in *Proc. IEEE Vehicular Technology Conference (VTC Spring)*, 2013, pp. 1–5.
[5] Z. Ding, X. Lei, G. K. Karagiannidis, R. Schober, J. Yuan, and V. K. Bhargava, "A survey on non-orthogonal multiple access for 5g networks: Research challenges and future trends," *IEEE J. Sel. Areas Commun.*, vol. 35, no. 10, pp. 2181–2195, Oct. 2017.
[6] Q. N. Le, N.-P. Nguyen, A. Yadav, and O. A. Dobre, "Outage performance of full-duplex overlay CR-NOMA networks with SWIPT," *accepted at the IEEE GLOBECOM, Waikoloa, HI, USA, 2019*, pp. 1–6.
[7] P. D. Diamantoulakis, K. N. Pappi, Z. Ding, and G. K. Karagiannidis, "Wireless-powered communications with non-orthogonal multiple access," *IEEE Trans. Wireless Commun.*, vol. 15, no. 12, pp. 8422–8436, Dec. 2016.
[8] P. D. Diamantoulakis, K. N. Pappi, G. K. Karagiannidis, H. Xing, and A. Nallanathan, "Joint downlink/uplink design for wireless powered networks with interference," *IEEE Access*, vol. 5, pp. 1534–1547, 2017.
[9] P. D. Diamantoulakis and G. K. Karagiannidis, "Maximizing proportional fairness in wireless powered communications," *IEEE Wireless Communications Letters*, vol. 6, no. 2, pp. 202–205, 2017.
[10] C. K. Vranas, P. S. Bouzinis, V. K. Papanikolaou, P. D. Diamantoulakis, and G. K. Karagiannidis, "On the gain of noma in wireless powered networks with circuit power consumption," *IEEE Communications Letters*, vol. 23, no. 9, pp. 1657–1660, 2019.
[11] B. Xia, Y. Fan, J. Thompson, and H. V. Poor, "Buffering in a three-node relay network," *IEEE Trans. Wireless Commun.*, vol. 7, no. 11, pp. 4492–4496, Nov. 2008.
[12] N. Zlatanov, R. Schober, and P. Popovski, "Buffer-aided relaying with adaptive link selection," *IEEE J. Sel. Areas Commun.*, vol. 31, no. 8, pp. 1530–1542, Aug. 2013.
[13] K. W. Choi and D. I. Kim, "Stochastic optimal control for wireless powered communication networks," *IEEE Trans. Wireless Commun.*, vol. 15, no. 1, pp. 686–698, Jan. 2016.
[14] M. J. Neely, "Stochastic network optimization with application to communication and queueing systems," *Synthesis Lectures on Communication Networks*, vol. 3, no. 1, pp. 1–211, 2010.
[15] Z. Li, Y. Jiang, Y. Gao, L. Sang, and D. Yang, "On buffer-constrained throughput of a wireless-powered communication system," *IEEE J. Sel. Areas Commun.*, vol. 37, no. 2, pp. 283–297, Feb. 2019.